

Common origin of insect trachea and endocrine organs from a segmentally repeated precursor

Carlos Sánchez-Higuera¹, Sol Sotillos¹ and James Castelli-Gair Hombría^{1*}.

¹CABD; CSIC/JA/Univ. Pablo de Olavide; Seville; 41013 Sevilla; Spain.

* Author for correspondence:

jcashom@upo.es

Telephone: 00-34-954348942

Fax: 00-34-954349376

Running title: Common origin of trachea and endocrine organs

Highlights:

- * We describe the developmental origin of the two main insect endocrine organs
- * We show the gene-network required for the development of insect endocrine organs
- * We introduce a novel model to study EMT and concerted cell migration
- * We uncover one of the most extreme cases of evolutionary organ divergence

Summary:

Segmented organisms have serially repeated structures [1] that become specialized in some segments [2]. We show that the *Drosophila corpora allata*, the prothoracic glands and the trachea have a homologous origin and can convert into each other. The tracheal epithelial tubes develop from ten trunk placodes [3, 4]; homologous ectodermal cells in the maxilla and labium, form the *corpora allata* and the prothoracic glands. The early endocrine and trachea gene networks are similar, with STAT and Hox genes inducing their activation. The initial invagination of the trachea and the endocrine primordia is identical, but activation of Snail in the glands induces an Epithelial to Mesenchymal Transition after which the *corpora allata* and prothoracic gland primordia coalesce and migrate dorsally joining the *corpora cardiaca* to form the ring gland. We propose that the Arthropod ectodermal endocrine glands and the respiratory organs arose through an extreme process of divergent evolution from a metameric repeated structure.

Results and discussion

The endocrine control of moulting and metamorphosis in insects is regulated by the *corpora allata* (*ca*) and the *prothoracic glands* (*pg*), which secrete Juvenile Hormone and Ecdysone respectively [5]. In diptera, these glands and the *corpora cardiaca* (*cc*) fuse during development to form a tripartite endocrine organ called the ring gland (Fig.1A). While the *corpora cardiaca* is known to originate from the migration of anterior mesodermal cells, the origin of the other two ring gland components is unclear [6, 7].

The tracheae have a completely different structure consisting of a tubular network of polarized cells [4]. The tracheae are specified in the second thoracic to the eighth abdominal segments (T2-A8) by the activation of *tracheiless* (*trh*) and *ventral veinless* (*vvl*) [4, 8-12].

We isolated the enhancers controlling *trh* and *vvl* in the tracheal primordia and showed they are activated by JAK/STAT signalling [13]. While the *trh* enhancers are restricted to the tracheal primordia in the T2 to A8 segments, the *vvl1+2* enhancer is also expressed in cells at homologous positions in the maxilla (Mx), labium (Lb), T1 and A9 segments in a pattern reproducing the early transcription of *vvl* (Fig.1C-E). The fate of these non-tracheal *vvl* expressing cells was unknown, but it was shown that ectopic *trh* expression transforms these cells into tracheae [14]. To identify their fate we made *vvl1+2-EGFP* and *mCherry* constructs. Although the *vvl1+2* enhancer drives expression transiently [13], the stability of the EGFP and mCherry proteins labels these cells during development. We observe that while the T1 and A9 patches remain in the surface and integrate with the embryonic epidermis, the patches in the Mx and Lb invaginate just as the tracheal primordia do (Fig.2N-N'). Next the Mx and Lb patches fuse and a group of them undergo an Epithelial to Mesenchymal Transition (EMT)

initiating a dorsal migration towards the anterior of the aorta where they integrate into the ring gland (Fig.2A-I and Fig.1F). To find out what controls the EMT we studied the expression of the *snail* (*sna*) gene, a key EMT regulator [15]. Besides its expression in the mesoderm primordium, we found that *sna* is also transcribed in two patches of cells that become the migrating primordium (Fig. S1A). Using *sna* BACs with different *cis*-regulatory regions [16-18] we localized the enhancer activating *sna* in the ring gland primordium (*sna-rg*). A *sna-rg-GFP* construct labels the subset of Mx and Lb *vv1+2* expressing cells that experience EMT and migrate to form the ring gland (Fig.2B-I, Movies S1-S2). Staining with *seven-up* (*svp*) and *spalt* (*sal*) [also known as *salm*] [19, 20] markers, that label the *ca* and the *pg* respectively (Fig.1B,G), shows that the *sna-rg-GFP* cells form these two endocrine glands (Fig.2K',M'). The *sna-rg-GFP* expressing cells in the Mx activate *svp* (Fig.2J) and those in the Lb activate *sal* (Fig.2L) before they coalesce, indicating that the *ca* and *pg* are specified in different segments before they migrate.

To test if Hox genes, the major regulators of antero-posterior segment differentiation [21], participate in gland morphogenesis we stained *vv1+2-GFP* embryos and found that the Mx *vv1+2* primordium expresses Deformed (*Dfd*) and the Lb primordium Sex combs reduced (*Scr*) while the T1 primordium expresses very low levels of *Scr* (Fig.3A). *Dfd* mutant embryos lack the *ca*, while *Scr* mutant embryos lack the *pg* (Fig.S2). *Dfd* and *Scr* expression in the gland primordia is transient suggesting they control their specification. Consistently, in *Dfd*, *Scr* double mutant embryos *vv1+2* is not activated in the Mx and Lb patches (Fig.3B) and the same is true for *vv1* transcription. In these mutants the *sna-rg-GFP* expression is almost absent (Fig.3C) and the *ca* and *pg* do not form. In each case *Dfd* controls the expression of the Mx patch and *Scr* of the Lb patch.

We tested the capacity of different Hox genes to rescue the ring gland defects of *Scr*, *Dfd* double mutants (Fig.3D,G,K,O and Fig.S3). Induction of *Dfd* with the *sal-Gal4* line in these mutants, restores the expression of *vv1+2* (Fig.3G) and *sna-rg-GFP* in the Mx and the Lb. However, in contrast to the wild type (Fig.2J-M), both segments form a *ca* as all cells express *Svp* (Fig.3E-F). Similarly, induction of *Scr* also restores the *vv1+2* (Fig.3K) and *sna-rg-GFP* expression but both primordia form a *pg* as they activate *Sal* and *phantom* [22], an enzyme required for ecdysone synthesis (Fig.3I-J). The capacity of both *Dfd* and *Scr* to restore *vv1* expression regardless of the segment, made us test if other Hox proteins could have the same function. Induction of *Antennapedia (Antp)*, *Ultrabithorax (Ubx)*, *abdominal-A (abd-A)* or *Abdominal-B (Abd-B)* restores *vv1+2* expression in the Mx and Lb, but these cells form tubes instead of migratory gland primordia (Fig.3L-O and Fig.S3). These cephalic tubes are trachea as they do not activate *sna-rg* (Fig.S3E'), express *Trh* and their nuclei accumulate Tango (Tgo), a maternal protein that is only translocated to the nucleus in salivary glands and tracheal cells [23], indicating that the trunk Hox proteins can restore *vv1* expression in the Mx and Lb, but induce their transformation to trachea.

To investigate if *vv1* and *trh* expression is normally under Hox control in the trunk, we focused on *Antp* that is expressed at high levels in the tracheal pits (Fig.S3J). In double *Dfd*, *Antp* mutant embryos (Fig.S3K-K') *vv1+2* is maintained in the Lb where *Scr* is present, while the Mx, T1 and T2 patches are missing. In T3-A8 *vv1+2* expression, although reduced, is present probably due to the expression of *Ubx*, *Abd-A* and *Abd-B* in the posterior thorax and abdomen. Thus, *Antp* regulates *vv1* expression in the tracheal T2 primordium. Surprisingly, in *Dfd*, *Antp* double mutants, *Trh* and *Tgo* are maintained in the T2 tracheal pit (Fig.S3K), indicating that although Hox genes can activate ectopic *trh* expression, in the tracheal primordia they may be acting redundantly

with some other unidentified factor, explaining why the capacity of Hox proteins to specify trachea had not been reported previously.

We studied *sna* null mutants to find out its requirement for ring gland development, but their aberrant gastrulation [24, 25] precluded analyzing specific ring gland defects. To investigate *sna* function in the gland primordia we rescued the *sna* mutants with the *sna-squish BAC* [16] that drives normal *Sna* expression except in the ring gland (Fig.S1B). These embryos have a normal gastrulation and activate the *sna-rg-GFP*, however the gland primordia degenerate and disappear (Fig.4B). To block apoptosis we made these embryos homozygous for the H99 deficiency that removes three apoptotic inducers [26]. In this situation, the *ca* and *pg* primordia invaginate and survive but they do not undergo EMT (Fig.4C). As a result the gland primordia maintain epithelial polarity, do not migrate and form small pouches that remain attached to the epidermis (Fig.4D).

Vvl is required for tracheal migration [8, 9, 27]. In *vvl* mutant embryos *sna-rg-GFP* expression is activated but the cells degenerate (Fig.4E). In *vvl* mutant embryos also mutant for H99, the primordia undergo EMT and migrate up to the primordia coalescence, however the later dorsal migration does not progress (Fig.4F-G).

We have shown that the *ca* and *pg* develop from *vvl* expressing cephalic cells at positions where other segments form trachea, suggesting that they could be part of a segmentally repeated structure that is modified in each segment by the activity of different Hox proteins. As the cephalic primordia are transformed into trachea by ectopic expression of trunk Hox (Fig.3L-N), we tested if the trachea primordia could form gland cells. Ectopic expression of *Dfd* with *arm-Gal4* results in the activation of *sna-rg-GFP* on the ventral side of the tracheal pits (not shown). These *sna-rg-GFP* expressing cells also express *vvl 1+2*, *Trh* and have nuclear *Tgo* showing that they

conserve tracheal characteristics. These *sna-rg-GFP* positive cells do not show EMT and keep associated to the ventral anterior tracheal branch. The strength of ectopic *sna-rg-GFP* expression increases when ectopic Dfd is induced in *trh* mutant embryos (Fig.3P). However migratory behaviours in the *sna-rg-GFP* cells are only observed if Dfd is coexpressed with Sal (Fig.3Q-T). Thus *sal* is expressed several times in the gland primordia, first at st9-10 repressing trunk Hox expression in the cephalic segments (Fig.S3G), and second from st11 in the prothoracic gland. It is uncertain if *sal* requirement for migration is linked to the first function or if it represents an additional role.

Our results show that the endocrine ectodermal glands and the respiratory trachea develop as serially homologous organs in *Drosophila*. The identical regulation of *vvl* in the primordia of trachea and gland by the combined action of the JAK/STAT pathway and Hox proteins (Fig.3, Fig.S3 and S4) could represent the vestiges of an ancestral regulatory network retained to specify these serially-repeated structures; while the activation of Sna for gland development, and Trh and Tgo for trachea formation could represent network modifications recruited later by specific Hox proteins during the functional specialization of each primordium (Fig.4H). This hypothesis or alternative possibilities should be confirmed by analyzing the expression of these gene networks in various arthropod species. The diversification of glands and respiratory organs must have happened before the split of Insects and Crustaceans as there is a correspondence between the endocrine glands in both Classes, with the *corpora cardiaca* corresponding to the pericardial organ; the *corpora allata* to the Mandibular organ; and the prothoracic gland to the Y-gland [5, 28, 29]. Despite their divergent morphology, a correspondence between the Insect trachea and the Crustacean gills can also be made, as both respiratory organs coexpress *vvl* and *trh* during their

organogenesis [30]. Divergence between endocrine glands and respiratory organs may have occurred when the evolution of the arthropod exoskeleton required solving two simultaneous problems: the need to moult to allow growth and the need of specialized organs for gas exchange.

Experimental Procedures

Constructs generated for this work:

A polylinker with EcoRI and XbaI restriction sites at the ends was synthesized (Sigma) and digested with EcoRI and XbaI. A pCaSpeR.lacZ.NLS was digested with EcoRI and XbaI, releasing the polylinker, the hs43 promoter and the lacZ.NLS that was substituted with the new polylinker creating (pCaSpeR polylinker) where a PH membrane domain from Phospholipase C delta digested with BamHI-XbaI, was cloned creating (pCaSpeR-PH). Next mCherry, was PCR amplified from pCS2+ vector, with BamHI/BglIII tailed primers. A sequenced mCherry PCR product was digested with BamHI-BglIII and cloned into pCaSpeR-PH BamHI digested (restriction site included in polylinker). Next, the hs43 promoter digested with BamHI-BglIII from pCaSpeR.NLS-LacZ, was cloned into BamHI, completing the plasmid pCaSpeR-mCherry-PH.

pCaSpeR-EGFP-PH, was constructed in a similar way using EGFP from the pCS2+ vector to create a pCaSpeR-EGFP-PH plasmid.

The *sna*-rg enhancer was amplified by PCR from *Drosophila* genomic DNA and cloned into pGEMTeasy using the following primers:

Upper *sna*-rg primer: 5'-ACCAAACCAGAACTCCAGACC-3'

Lower *sna*-rg primer: 5'- GCTTGGGTTTTTCGTTTTTCAG-3'

Finally, the enhancer was subcloned into pCaSpeR-EGFP-PH to create a reporter plasmid. The *vvl 1+2* enhancer [13] was cloned from pGEMT-easy to pCaSpeR-mCherry-PH and pCaSpeR-EGFP-PH reporter plasmids. Both plasmids were transformed into *Drosophila* by the *Drosophila* Consolider-Ingenio 2007 transformation platform (Spain).

Fly stocks

The following mutant alleles and transgenic lines from the *Drosophila* Bloomington stock collection were used:

Dfd^d ; *Dfd^{d6}*, *Scr^d* ; *Df(3L)H99*; *Df(1)os1A*; *Dfd^{d6}* , *Antp⁷*; *P{HZ}svp³*; *vvl^{GA3}*; *trh⁸*; *sna¹*; *sna¹⁸*; *P{UAS-Dfd.B}W4*; *P{UAS-Scr.M}EE2*; *P{UAS-Antp.Mb}W1*; *P{UAS-myr-mRFP}*. *UAS-sal* and *Df(2)5 sal sal^r* were obtained from R. Barrio, and *phm-*

GAL4>CD8::GFP line [31] from Marco Milán. The *sna-lacZ* 6kb reporter and *sna-GFP BAC* collection was obtained from A. Stathopoulos and M. Levine. The following stocks from our laboratory were used: *UAS-Ubx*; *UAS-AbdBm* [32]; the reporter *vvl1+2-lacZ*; and the enhancer trap lines *sal-GAL4 459.2* and *arm-Gal4* (Bloomington stock number 1560).

Primary antibodies: Chicken anti-gfp (Abcam); rabbit anti-gfp (Invitrogen); rat anti-RFP (Chromotek); rabbit or mouse anti-βGal (Promega) and Chicken anti-βGal (Abcam); rat anti-Trh (J. Casanova); rabbit anti-Sal (R. Barrio); rabbit anti-Svp (R.

Cripps); rabbit anti-aPKC (Santa Cruz); rabbit anti-Dfd (T. Kaufman); anti-DIG-AP (Roche) and from the Hybridoma Bank we obtained mouse anti-Tgo; mouse anti-Fas II; mouse anti-Scr; mouse anti-AbdB; mouse anti-Ubx (FP3.38) and mouse anti-Antp.

Secondary antibodies: The following Invitrogen antibodies were used: anti-mouse A488; anti-mouse A555; anti-mouse A647; anti-chicken A488; anti-Goat A647; anti-Rabbit A488; anti-Rabbit A555; anti-Rabbit A647 and anti-Rat A555.

RNA probes: In situ RNA probes: *snail* RE35237 and *phantom* RE03155. Riboprobes were made using DIG RNA Labeling Kit (Roche).

Microscopy:

In vivo time-lapse microscopy was done using a Leica DMI 6000 SP5 MP-AOBS inverted confocal microscope. A Leica SPE Confocal Microscope was used for multiple antibody stainings and in situ/antibody stainings. Images were processed using ImageJ and Imaris (7.6).

Acknowledgements

We thank M. Averof, J. Casanova, J. Culi, B. Denholm, J.R. Martínez-Morales and E. Sánchez-Herrero for critical reading of the manuscript; and R. Barrio, J. Casanova, R.M. Cripps, T.C. Kaufman, M. Levine, A. Stathopoulos for antibodies and reagents. S.S. is a Ramón y Cajal Fellow. This work was supported by grants of the Programa Consolider, the Junta de Andalucía and the Spanish MICINN/FEDER to J.C-G. H.

REFERENCES

1. Davis, G.K., and Patel, N.H. (1999). The origin and evolution of segmentation. *Trends Cell Biol* 9, M68-72.
2. Hueber, S.D., and Lohmann, I. (2008). Shaping segments: Hox gene function in the genomic age. *Bioessays* 30, 965-979.
3. Ghabrial, A., Luschnig, S., Metzstein, M.M., and Krasnow, M.A. (2003). Branching morphogenesis of the *Drosophila* tracheal system. *Annu Rev Cell Dev Biol* 19, 623-647.
4. Manning, G., and Krasnow, M.A. (1993). Development of the *Drosophila* tracheal system. In *The Development of Drosophila melanogaster*, Volume 1, B. M. and M.-A. A., eds. (Cold Spring Harbor, NY: Cold Spring Harbor Laboratory Press), pp. 609-685.
5. Hartenstein, V. (2006). The neuroendocrine system of invertebrates: a developmental and evolutionary perspective. *J Endocrinol* 190, 555-570.
6. De Velasco, B., Shen, J., Go, S., and Hartenstein, V. (2004). Embryonic development of the *Drosophila* corpus cardiacum, a neuroendocrine gland with similarity to the vertebrate pituitary, is controlled by *sine oculis* and *glass*. *Dev Biol* 274, 280-294.
7. Park, S., Bustamante, E.L., Antonova, J., McLean, G.W., and Kim, S.K. (2011). Specification of *Drosophila* corpora cardiaca neuroendocrine cells from mesoderm is regulated by Notch signaling. *PLoS Genet* 7, e1002241.
8. Anderson, M.G., Perkins, G.L., Chittick, P., Shrigley, R.J., and Johnson, W.A. (1995). *drifter*, a *Drosophila* POU-domain transcription factor, is required for correct differentiation and migration of tracheal cells and midline glia. *Genes Dev* 9, 123-137.
9. de Celis, J.F., Llimargas, M., and Casanova, J. (1995). *Ventral veinless*, the gene encoding the Cfla transcription factor, links positional information and cell differentiation during embryonic and imaginal development in *Drosophila melanogaster*. *Development* 121, 3405-3416.
10. Isaac, D.D., and Andrew, D.J. (1996). Tubulogenesis in *Drosophila*: a requirement for the *trachealess* gene product. *Genes Dev* 10, 103-117.
11. Wilk, R., Weizman, I., and Shilo, B.Z. (1996). *trachealess* encodes a bHLH-PAS protein that is an inducer of tracheal cell fates in *Drosophila*. *Genes Dev* 10, 93-102.
12. Kerman, B.E., Cheshire, A.M., and Andrew, D.J. (2006). From fate to function: the *Drosophila* trachea and salivary gland as models for tubulogenesis. *Differentiation* 74, 326-348.
13. Sotillos, S., Espinosa-Vazquez, J.M., Foglia, F., Hu, N., and Hombria, J.C. (2010). An efficient approach to isolate STAT regulated enhancers uncovers STAT92E fundamental role in *Drosophila* tracheal development. *Dev Biol* 340, 571-582.
14. Boube, M., Llimargas, M., and Casanova, J. (2000). Cross-regulatory interactions among tracheal genes support a co-operative model for the induction of tracheal fates in the *Drosophila* embryo. *Mech Dev* 91, 271-278.

15. Thiery, J.P., Acloque, H., Huang, R.Y., and Nieto, M.A. (2009). Epithelial-mesenchymal transitions in development and disease. *Cell* *139*, 871-890.
16. Dunipace, L., Ozdemir, A., and Stathopoulos, A. (2011). Complex interactions between cis-regulatory modules in native conformation are critical for *Drosophila* snail expression. *Development* *138*, 4075-4084.
17. Ip, Y.T., Park, R.E., Kosman, D., Yazdanbakhsh, K., and Levine, M. (1992). dorsal-twist interactions establish snail expression in the presumptive mesoderm of the *Drosophila* embryo. *Genes Dev* *6*, 1518-1530.
18. Perry, M.W., Boettiger, A.N., Bothma, J.P., and Levine, M. (2010). Shadow enhancers foster robustness of *Drosophila* gastrulation. *Curr Biol* *20*, 1562-1567.
19. Barrio, R., de Celis, J.F., Bolshakov, S., and Kafatos, F.C. (1999). Identification of regulatory regions driving the expression of the *Drosophila* spalt complex at different developmental stages. *Dev Biol* *215*, 33-47.
20. Ryan, K.M., Hoshizaki, D.K., and Cripps, R.M. (2005). Homeotic selector genes control the patterning of seven-up expressing cells in the *Drosophila* dorsal vessel. *Mech Dev* *122*, 1023-1033.
21. Pearson, J.C., Lemons, D., and McGinnis, W. (2005). Modulating Hox gene functions during animal body patterning. *Nat Rev Genet* *6*, 893-904.
22. Warren, J.T., Petryk, A., Marques, G., Parvy, J.P., Shinoda, T., Itoyama, K., Kobayashi, J., Jarcho, M., Li, Y., O'Connor, M.B., Dauphin-Villemant, C., and Gilbert, L.I. (2004). Phantom encodes the 25-hydroxylase of *Drosophila melanogaster* and *Bombyx mori*: a P450 enzyme critical in ecdysone biosynthesis. *Insect Biochem Mol Biol* *34*, 991-1010.
23. Ward, M.P., Mosher, J.T., and Crews, S.T. (1998). Regulation of bHLH-PAS protein subcellular localization during *Drosophila* embryogenesis. *Development* *125*, 1599-1608.
24. Alberga, A., Boulay, J.L., Kempe, E., Dennefeld, C., and Haenlin, M. (1991). The snail gene required for mesoderm formation in *Drosophila* is expressed dynamically in derivatives of all three germ layers. *Development* *111*, 983-992.
25. Grau, Y., Carteret, C., and Simpson, P. (1984). Mutations and Chromosomal Rearrangements Affecting the Expression of Snail, a Gene Involved in Embryonic Patterning in *DROSOPHILA MELANOGASTER*. *Genetics* *108*, 347-360.
26. White, K., Grether, M.E., Abrams, J.M., Young, L., Farrell, K., and Steller, H. (1994). Genetic control of programmed cell death in *Drosophila*. *Science* *264*, 677-683.
27. Zelzer, E., and Shilo, B.Z. (2000). Interaction between the bHLH-PAS protein Tracheless and the POU-domain protein Drifter, specifies tracheal cell fates. *Mech Dev* *91*, 163-173.
28. Chang, E.S., and O'Connor, J.D. (1977). Secretion of alpha-ecdysone by crab Y-organs in vitro. *Proc Natl Acad Sci U S A* *74*, 615-618.
29. Laufer, H., Borst, D., Baker, F.C., Reuter, C.C., Tsai, L.W., Schooley, D.A., Carrasco, C., and Sinkus, M. (1987). Identification of a Juvenile Hormone-Like Compound in a Crustacean. *Science* *235*, 202-205.
30. Franch-Marro, X., Martin, N., Averof, M., and Casanova, J. (2006). Association of tracheal placodes with leg primordia in *Drosophila* and implications for the origin of insect tracheal systems. *Development* *133*, 785-790.
31. Ono, H., Rewitz, K.F., Shinoda, T., Itoyama, K., Petryk, A., Rybczynski, R., Jarcho, M., Warren, J.T., Marques, G., Shimell, M.J., Gilbert, L.I., and

- O'Connor, M.B. (2006). Spook and Spookier code for stage-specific components of the ecdysone biosynthetic pathway in Diptera. *Dev Biol* 298, 555-570.
32. Castelli-Gair, J. (1998). Implications of the spatial and temporal regulation of Hox genes on development and evolution. *Int J Dev Biol* 42, 437-444.
33. Hombria, J.C., Brown, S., Hader, S., and Zeidler, M.P. (2005). Characterisation of Upd2, a *Drosophila* JAK/STAT pathway ligand. *Dev Biol* 288, 420-433.

Figure legends

Figure 1. Ring gland structure and primordia origin. (A) Frontal view reconstruction of a late embryo ring gland showing the position of the three independent glands: The *corpora allata* (green) expresses *svp*, the prothoracic glands (red) *phantom*, and the *corpora cardiaca* (blue) is labelled by FasII. (B) Dorsal view of a late embryo labelled with *sal-Gal4* driving *UAS-RFP* and *svp-lacZ*. The ring gland is localized anterior to the aorta (note that *svp* also labels some cardiomyocytes in the aorta and heart (yellow asterisk)). (C) At extended germ band *vv11+2-EGFP* labels the tracheal primordia in T2-A8 as well as cells in more anterior and posterior segments. (D) Expression of the Trh protein in the ten tracheal primordia as well as the salivary gland. (E) Double staining of *vv11+2* and Trh. (F) Frontal view of a ring gland in the process of fusing dorsally stained with FasII and *vv11+2-EGFP*, the *corpora allata* and the prothoracic glands express *vv11+2* showing their ectodermal origin, while the *corpora cardiaca* does not. (G) Ring gland z-section of a *sal-Gal4 UAS-RFP, svp-lacZ* embryo stained with RFP, anti-bgal and FasII. Images from this series were used for the reconstruction shown in (A). White scale bar 50µm, yellow scale bars 10µm.

Figure 2. Formation of the *corpora allata*, prothoracic glands and tracheae. (A-I) Embryos double stained to detect the *vv11+2-mCherry* marking gland and trachea (red), and the *sna-rg-EGFP* (green) marking the corpora allata and prothoracic glands. (A) Early st10 embryos express *vv11+2* in a segmentally repeated pattern. (B) In st11 embryos *vv11+2* cells invaginate in all segments except in T1 and A9. In the Mx and Lb a subgroup of *vv11+2* cells activate *sna-rg-EGFP*. (C) Tracheal primordia from T2 to A8 start branching at the time when the *sna-rg-EGFP* cells experience the Epithelial to

Mesenchymal Transition. (D) Dorsal migration of the coalesced *ca/pg* primordium, all migrating cells express *sna-rg-EGFP* while non-snail expressing *vv11+2* cells stay behind. (E-G) Close-up of the Mx and Lb segments before (E-F) and after (G) the two gland primordia coalesce. Note that there are two different coalescence processes: one at st11 when the *vv11+2* expressing cells invaginating from the Mx and Lb come together (F); another, at st13 when the migrating *sna-rg-EGFP* cells coalesce (G). (H) Dorsal view of the *sna-rg-EGFP* cells at the time when the prothoracic glands meet the *corpora cardiaca* (unstained in this figure). (I) Dorsal view of the ring gland as the contralateral *corpora allata* primordia fuse (comparable frontal view in Fig.1F-G). (J-M) Specification of the *corpora allata* and prothoracic glands. (J) *svp-lacZ*, *sna-rg-EGFP* embryos double stained with anti-βgal and anti-GFP show that the *corpora allata* is specified in the Mx prior to coalescence and maintains *svp* expression until the ring gland is formed (K-K'). (L) *sna-rg-EGFP* cells double stained using anti-Spalt to show that the prothoracic gland is specified in the Lb before coalescence. (M-M') Embryo expressing *sal-Gal4* showing that this line drives expression specifically in the prothoracic gland. (N-N') Embryos double stained for *vv11+2* and aPKC show that both the gland primordia (N) and the trachea primordia (N') maintain epithelial polarity during invagination. (O-O') In the Mx and Lb segments only *vv11+2* cells expressing *sna-rg-EGFP* experience EMT and lose apical aPKC; in contrast, *vv11+2* cells never lose apical polarity in the trachea (P). Asterisk in g and o labels *vv11+2* cells that do not activate *sna* and maintain epithelial characteristics. White scale bar 50μm, yellow scale bars 10μm, purple scale bars 25μm. (See also Fig. S1 and Movies S1-S2).

Figure 3. Hox genes control the specification of *corpora allata*, prothoracic glands and trachea. (A) Ventral view of a *vv11+2-EGFP* embryo stained with anti-Dfd (blue)

and anti-Scr (red). (B-C) *Dfd*, *Scr* double mutant embryos fail to activate *vv11+2* in the Mx and Lb (B, asterisks) and have very low levels of *sna-rg* (C). (D,G,K,O) *Dfd*, *Scr* double mutants expressing GFP or different Hox genes with the *sal-Gal4* line that drives early expression in the Mx, Lb and T1 segments (D). (D-D') Expression of GFP does not rescue *vv11+2* expression (red) in *Dfd*, *Scr* mutant embryos. Expression of *Dfd* (G), *Scr* (K) or *Antp* (O) rescues *vv11+2* expression in both Mx and Lb (asterisks). (E-F) Embryos rescued with *Dfd* produce ring glands composed exclusively of *corpora allata* cells as judged by *Svp* expression. (H-H'') Wild type ring glands express *phm* only in the subset of *sna-rg* cells forming the prothoracic gland. (I-I'') Embryos rescued with *Scr* produce ring glands composed exclusively of prothoracic gland cells as judged by *phm* or (J) *sal-Gal4* expression in all the *sna-rg* cells. (L) *Dfd*, *Scr* embryo rescued with *Antp* show nuclear Tgo in the cephalic segments. (M-M'') Close up of an embryo of the same genotype as in (L) showing the *vv11+2* primordium in the Mx is transformed towards trachea as it expresses Tango. (N-N') *Dfd*, *Scr* embryo rescued with *Antp* induces expression of *Trh* in the head indicating they are forming trachea. (P) Ectopic expression of *Dfd* in the ectoderm using the *arm-Gal4* line induces robust expression of *sna-rg-EGFP* in the trunk segments of *trh* mutant embryos. (Q-T) Embryos labelled with *vv11+2 mCherry* and expressing *Dfd* and *Sal* with the *arm-Gal4* line induce the expression of *sna-rg-EGFP* in a ventral subset of *vv11+2* cells (Q); the *sna-rg-EGFP* cells become motile (R-R') migrating dorsally (S-T). Note that despite the UAS-*Scr* line (K) expressing lower amounts of protein than other Hox lines used (G,O), these are sufficient to rescue *vv11+2* expression. White scale bars 50µm, yellow scale bars 10µm. (See also Fig. S2 and S3 S4).

Figure 4. Function of Sna and Vvl in the ring gland. (A) Wild type *ca* and *pg* primordia labelled with *sna-rg-GFP* at st11. (B) The *ca* and *pg* become apoptotic and disintegrate when *sna* is removed specifically from the primordia. (C) When apoptosis is blocked from *ca* and *pg* primordia that do not express Sna, the cells do not go into EMT and remain attached to the surface without losing apical aPKC (purple). (D) *ca* and *pg* primordia not expressing Sna do not migrate and the primordia remain separated at late stages. (D') Close up of the *pg* in (D) showing that the primordium's apical side integrates with the neighbouring epithelial cells. (E) In *vvl* mutant embryos the ring gland primordia also become apoptotic. (F-G) *vvl* mutant embryos where apoptosis is prevented by the deletion of the apoptotic inducers. The *ca* and *pg* invaginate and go into EMT losing apical aPKC. Although both primordia coalesce (G) dorsal migration does not progress. (H) Schematic representation of the early ectodermal endocrine and respiratory primordia specification gene-network. In both networks Hox and STAT induce the expression of the early transcription factors. While all Hox genes can induce *vvl* expression only Dfd and Scr induce *sna* expression, while trunk Hox genes induce Trachealess expression. Sal represses trunk Hox expression in the head (H) preventing *trh* expression. White scale bar 50µm, yellow scale bars 10µm (See also Fig. S4).

Supplemental information

Figure S1. Related to Figure 2. *sna* expression in the corpora allata and prothoracic gland. (A) *In situ sna* mRNA expression during embryogenesis. At blastoderm (st4) *sna* is activated in the mesoderm primordium, this expression soon disappears with *sna* becoming activated at st11 in specific cells including the ca and pg primordia (asterisks) before coalescence. Expression of *sna* is maintained during dorsal migration (st13) and ceases just before dorsal fusion (red asterisks show wing and haltere *sna* expression appearing as ring gland expression fades away at st15). Schematic representation of the genomic *sna* region including part of the neighbouring *Tim17b2* gene, and the constructs and BAC elements used to localize the *sna*-ring gland enhancer. (C) Summary of ring gland activity of the different constructs. The Full upstream BAC and the BAC element deleting both distal and proximal shadow mesoderm enhancers maintain ring gland expression. The *sna* SQUISH BAC lacks ring gland expression but is capable of rescuing the germ band abnormalities of *sna* null mutant embryos without rescuing *sna* function in the ring gland. These data and the expression of a 6kb *sna-lacZ* reporter gene in the ring gland primordia, locates the region controlling *sna* expression in the ring gland to a 1.9 kb fragment. (D) Expression of the *sna-rg* enhancer drives strong levels of EGFP in the *corpora allata* and the prothoracic glands from st11 up to larval stages.

Figure S2. Related to Figure 3. Hox gene requirement for *corpora allata* and prothoracic gland development. Dorsal views of late *syp-lacZ* embryos stained with anti- β GAL (green) and a *phm* RNA probe (purple) to show the *corpora allata* and prothoracic gland in wild type (A), *Dfd* (B) or *Scr* mutant embryos (C). In the dorsal

region focused here, *svp-lacZ* also labels four cardiomyocytes per segment in the aorta. In these stainings there is some unspecific labelling of the tracheal lumen. In *Dfd* mutants the corpora allata do not form (B) but the prothoracic glands (B') develop normally. In *Scr* mutants the prothoracic glands do not form (C) but the corpora allata reach their normal destination (C'). Yellow scale bars 10 μ m.

Figure S3. Related to Figure 3. Capacity of Hox genes to activate tracheal and ring gland markers. (A) In a *Dfd, Scr* double mutant embryo, ectopic expression of Ubx (blue) with a *sal-Gal4* line rescues expression of *vv11+2* (red) in the Mx and Lb (asterisks in A') and also induces ectopic Trh expression (purple in the close up shown in B). (C) Ectopic Abd-B expression (green) also rescues *vv11+2* expression (red in C and C') in the Mx and Lb (asterisks in C') and induces ectopic Trh expression (purple in D). (E) Ectopic Ubx expression rescues *vv11+2* expression but does not induce *sna-rg-EGFP* (E' asterisks). (F) In a wild type embryo, ectopic Antp expressed with *sal-Gal4* induces anterior Trh expression in T1 and Mx but does not eliminate the *sna-rg* expression driven by cephalic Hox genes (asterisks). (G-H) In *sal* mutant embryos there is ectopic Ubx expression (G) correlating with the formation of ectopic trachea observed in these embryos as shown by nuclear Tgo localization (H). (I) Ectopic expression of Ubx with *sal-Gal4* induces trachea formation in T1 but not in the Mx and Lb segments probably due to endogenous *Dfd* and *Scr* expression in these segments (compare with B). (J) *vv11+2-EGFP* embryos costained with Antp (red) show high Antp expression in the T2 tracheal pit and moderate levels in T1. (K-K') In *Dfd, Antp* double mutant embryos *vv11+2* expression (red) is reduced from the Mx, T1 and T2 segments correlating with the domains where *Dfd* and Antp proteins should be expressed. High levels of *vv11+2* expression are maintained in the Lb where *Scr* is

expressed. Intermediate levels of *vv11+2* expression are observed in T3-A5, which is the domain of Ubx and Abd-A expression. High levels of *vv11+2* are present in the Abd-B expression domain. Tgo nuclear localization (green in K) is not affected in the T2 tracheal primordium despite the absence of Antp indicating that there is another mechanism to maintain Trh/Tgo expression in trunk segments besides the Hox proteins. White scale bars 50µm, purple scale bars 25µm.

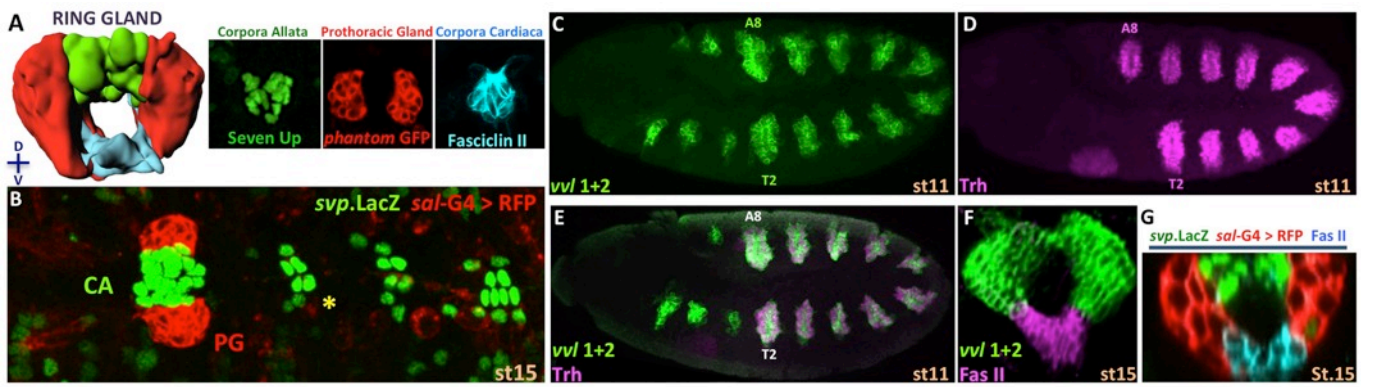
Figure S4. Related to Figure 4. JAK/STAT signalling requirement for Sna and Vvl expression in the ring gland and tracheae primordia. (A) Wild type embryo expressing *sna-rg* (green) and *vv11+2* (red in A'). (B) *Df(1)os1A* embryos lacking all three upd ligands required for JAK/STAT activation[33] show reduced *sna-rg* expression (asterisks in B) and *vv11+2* expression (red in B'). White scale bars 50µm.

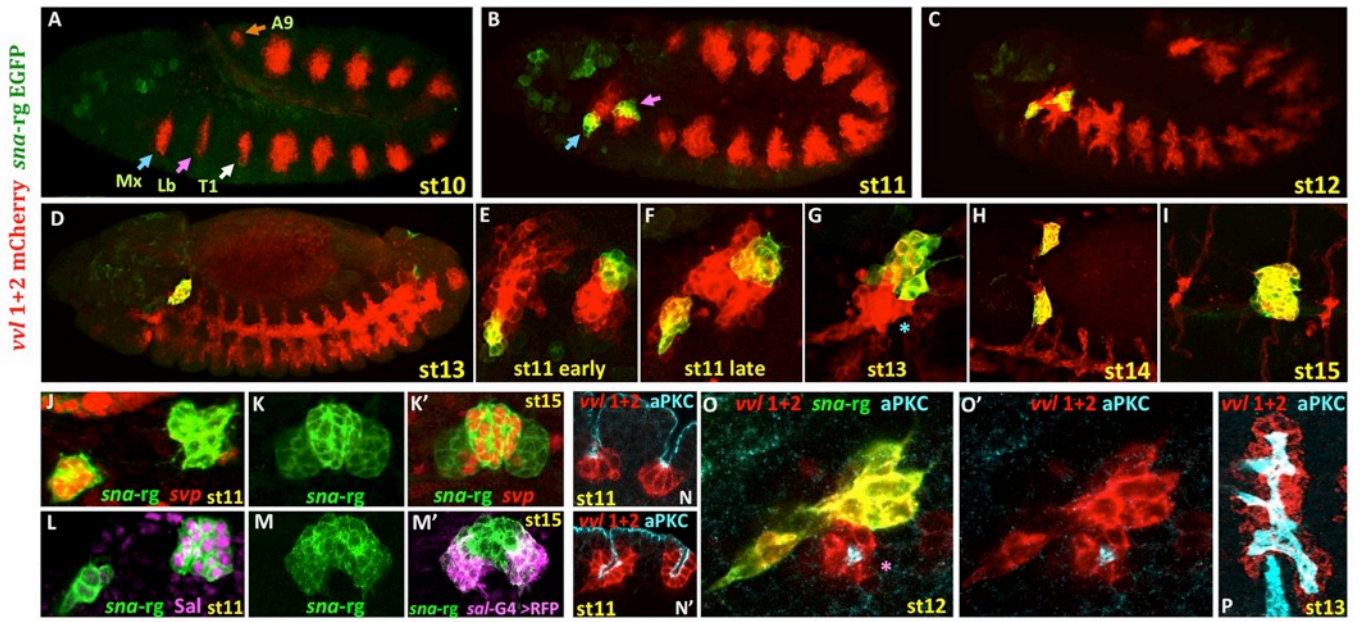
Supplementary movie 1. Primordia coalescence and dorsal migration.

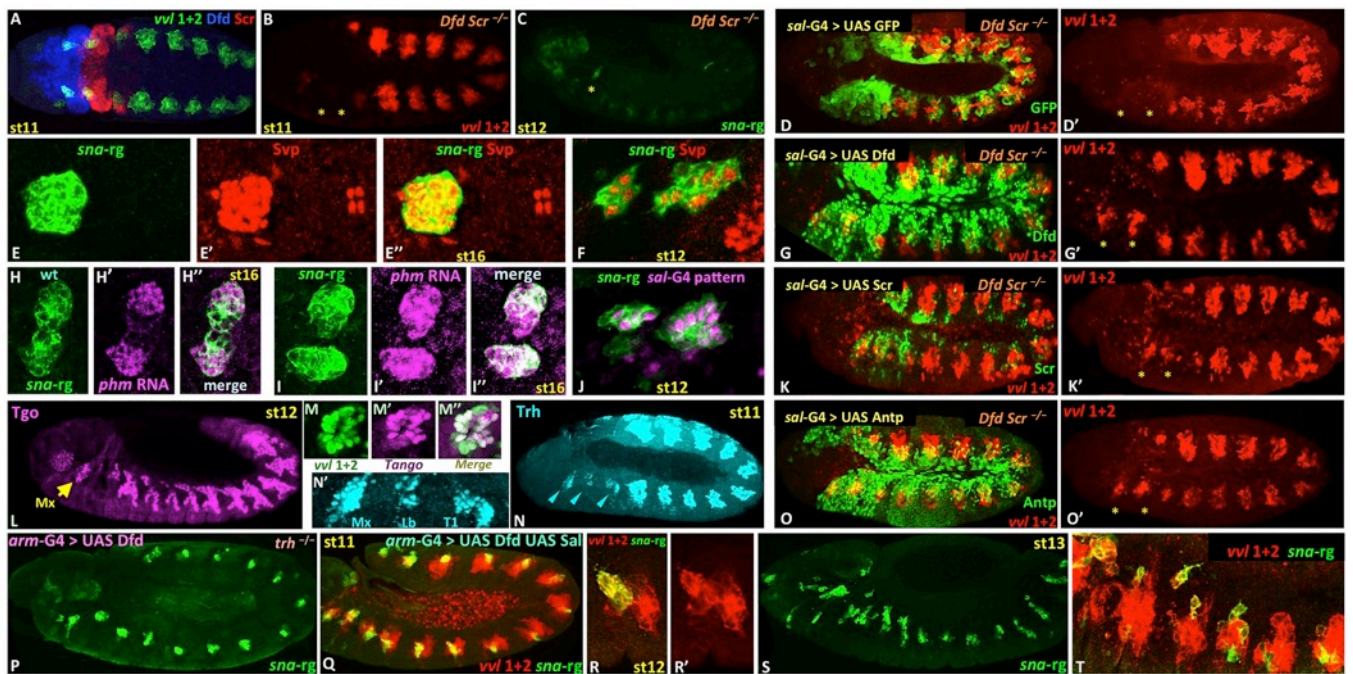
Lateral view of st11 to st14 *sna-rg-EGFP* homozygous embryos showing the coalescence and dorsal migration of the *corpora allata* and the prothoracic gland. Scale bar 50µm.

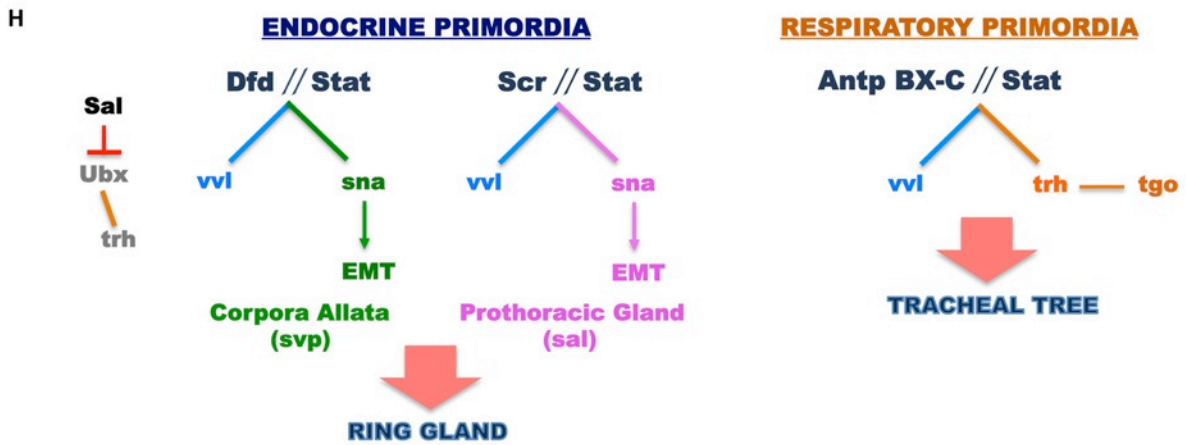
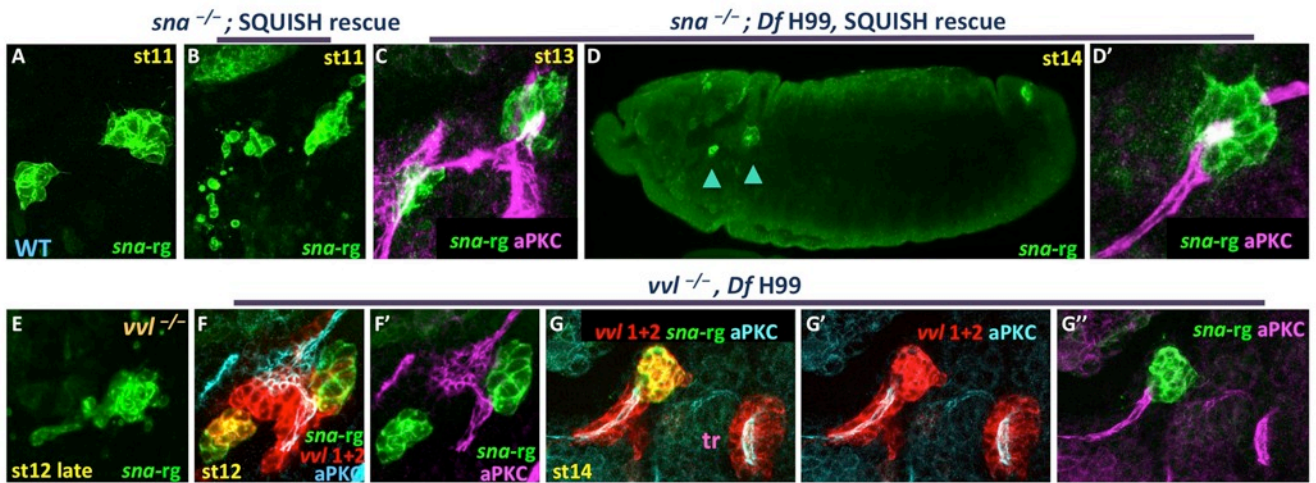
Supplementary movie 2. Ring gland dorsal fusion.

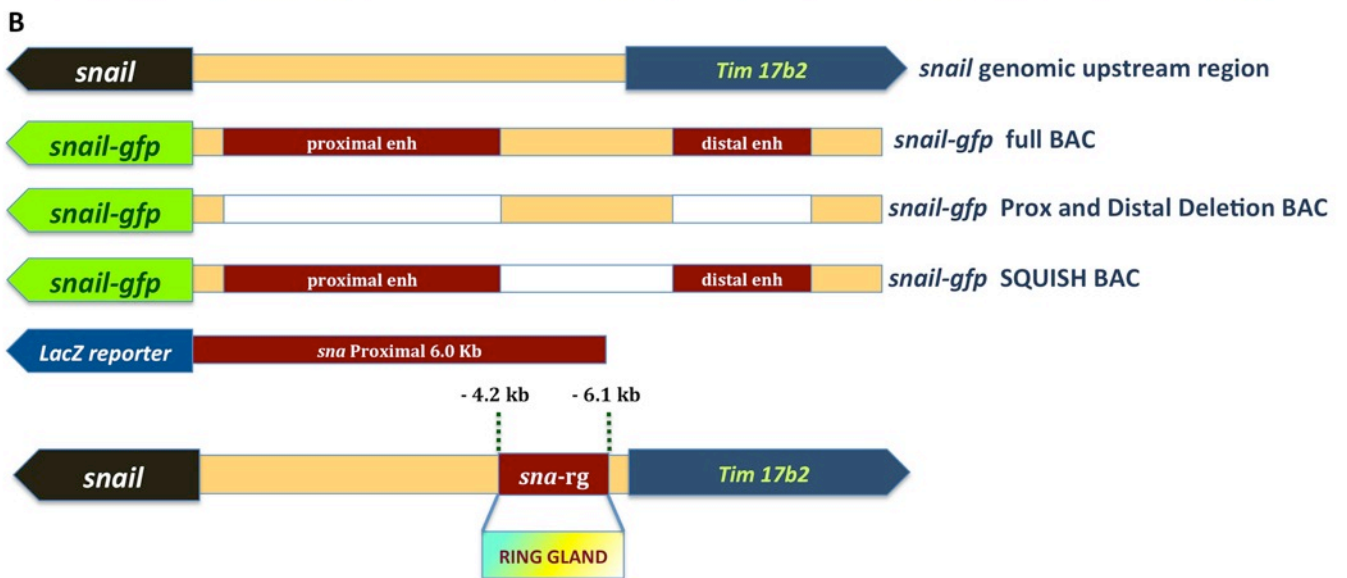
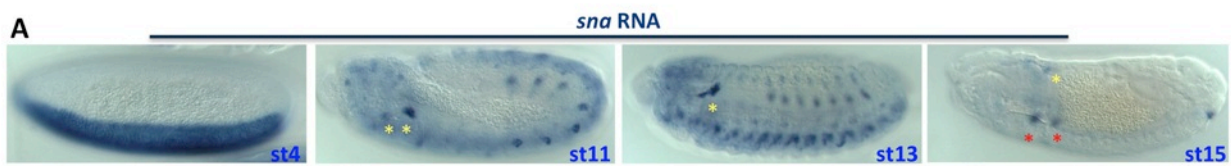
Dorsal view of st14 to st15 *sna-rg-EGFP* homozygous embryos showing the fusion of the contralateral *corpora allata*. Note the active formation of filopodia. Scale bar 10µm.











C

Gene Construct	Ring Gland Expression
<i>snail-gfp</i> Full BAC	Positive
<i>snail-gfp</i> Proximal and Distal Deletion BAC	Positive
<i>snail-gfp</i> SQUISH BAC	Negative
<i>sna</i> Proximal 6.0 Kb LacZ	Positive

